Thin Solid Films 763 (2022) 139581

Contents lists available at ScienceDirect

Thin Solid Films

journal homepage: www.elsevier.com/locate/tsf

Calibration of achromatic Fresnel rhombs with an elliptical retarder model in Mueller matrix ellipsometers

Subiao Bian [a,b,c], Xipeng Xu [a,b], Changcai Cui [a,b,*], Oriol Arteaga [c,d,**]

[a] Institute of Manufacturing Engineering, Huaqiao University, Xiamen 361021, China
[b] National and Local Joint Engineering Research Center for Intelligent Manufacturing Technology of Brittle Material Products, Huaqiao University, Xiamen 361021, China
[c] Dep. Fisica Aplicada, Plat Group, Universitat de Barcelona, Barcelona 08028, Spain
[d] Institute of Nanoscience and Nanotechnology (IN2UB), Universitat de Barcelona, Barcelona 08028, Spain

ARTICLE INFO

Keywords:
Mueller matrix ellipsometer
Fresnel rhomb
Stress
Calibration
Systematic error

ABSTRACT

Fresnel rhombs are the most achromatic form of retarders available and they are suitable compensating elements for spectroscopic Mueller matrix ellipsometers. However, the small stress in the rhomb caused by the mount or produced during the fabrication can affect the ellipsometry measurements with non-negligible systematic errors, due to the relatively long path length of light inside the rhomb. This work describes a calibration method that considers the non-ideal response of the Fresnel rhomb, and that it is especially well suited for calibrating Mueller matrix ellipsometers. The method describes each rhomb as the most general form of an elliptical retarder with a small ellipticity, instead of simply assuming that they behave as linear retarders. After this calibration, we show that the systematic errors of measurements are significantly decreased.

1. Introduction

The Fresnel rhomb is an optical prism that produces phase differences between two perpendicular components of polarization by means of total internal reflections. It was pioneered by Fresnel during 1820’s [1] and it was essential for his complete understanding of the polarization of light. Fresnel rhombs provide the most achromatic retardation response and they have been utilized in the fields of interferometry [2], 3D printing [3], ellipsometry [4] etc. They are made from optical isotropic materials such as glass BK7, CaF_2, fused silica, ZnSe that do not change light polarization state when light propagates through the medium, as opposed to what happens to plates based on birefringent effects. The achromatic retardance is attributed to several total internal reflections where the light is incident at a sufficiently oblique angle on the interface and then phase shifts between orthogonal electric field components (s and p components of the light beam) [5]. The value of retardance can be precisely controlled by the design of the number and incident angle of total internal reflection inside Fresnel rhombs.

For applications that use light beams with a diameter of one or several mm, Fresnel rhombs usually require prisms with an overall length of several centimeters, and to avoid lateral beam displacements it is common to use a “V” shaped design, that uses two equal prisms optically contacted. As a result, light travels a long path inside the prism and this makes them more vulnerable to extra stress-induced birefringence arising either from fabrication or from mounting [6]. The retardance arising from stress-induced birefringence is

$$\delta_t = 2\pi d \Delta / \lambda \tag{1}$$

where, δ_t represents the value of the accumulated stress-induced retardance, d represents the length of the beam path, Δ is relative to the stress and stress-optic coefficients of the medium [7], λ is the wavelength of the light in vacuum. According to Eq. (1), even if very weak stress occurs inside the Fresnel rhomb (very small Δ), it may have a significant effect on δ_t because the overall beam path, d, is much larger than the wavelength. Accordingly, in addition to the accumulated retardance coming from total internal reflections, it is often necessary to consider also the retardance coming from propagation in the slightly stressed optical material.

The change in polarization induced by a Fresnel rhomb can be expressed in terms of the Mueller matrix. This 4 × 4 real matrix is the most general description of linear optical phenomenons that involve polarization transformations. A non-depolarizing Mueller matrix also called Mueller–Jones Matrix can be described in terms of eight parameters, which can be derived from Jones differential calculus [8].

* Correspondence to: Institute of Manufacturing Engineering, Huaqiao University, Xiamen 361021, China.
** Correspondence to: Física Aplicada i Òptica Department and IN2UB, C/ Martí i Franquès 1, Universitat de Barcelona, Catalonia, Spain.
E-mail addresses: cuichc@hqu.edu.cn (C. Cui), oarteaga@ub.edu (O. Arteaga).

https://doi.org/10.1016/j.tsf.2022.139581
Received 29 August 2022; Received in revised form 24 October 2022; Accepted 3 November 2022
Available online 8 November 2022

Recently, the stress-induced linear birefringence generated in a "K" shaped Fresnel rhomb was analyzed by means of a model based on a cascaded multiplication of Mueller matrix [9]. The rhomb was effectively decomposed into interfaces and bulk propagation regions and each part was modeled by its own independent Mueller matrix.

In our previous work [10], we employed "V"-shaped Fresnel rhombs as compensators in our home-built Mueller matrix ellipsometer, which provide retardance values close to the optimal 132° making measurements with an optimal robustness level. However, in that work, the Fresnel rhombs were treated with a linear retarder model, which essentially neglects stress-induced birefringence effects. The measurement of this system included some small systematic errors that emerged from stress-induced birefringence effects in the rhomb, as they essentially depended on the pressure applied to hold the prisms in place in their holder.

In this work, a Fresnel rhomb is described as the most general form of an elliptical retarder with a small ellipticity, instead of simply assuming they behave as a linear retarder in the spectroscopic calibration process of a Mueller matrix ellipsometer. The advantage of this method is that despite it uses one single Mueller matrix to describe the rhomb, it takes into consideration all optical properties (even those that result from non-idealities) the most significant ones being the values of linear retardance, optical rotation, and azimuthal angle. In this work, we also evaluate how small interface-induced linear and circular diattenuation effects can further improve the calibration of an ellipsometer based on dual rotating Fresnel rhomb compensators.

2. Theory description

The Mueller matrix ellipsometer is composed of a train of optical elements that can be described by the Stokes–Mueller calculus. The measurement process is described by a matrix product representing the sequence of optical elements in the instrument. Light with Stokes vector $\mathbf{S_{in}}$, passes first through a polarizer, $\mathbf{P}_0$, and then goes through the first rotating compensator, $\mathbf{M}_{C0}$. After being transmitted through or reflected from the sample, $\mathbf{M}_S$, it goes through the second rotating compensator, $\mathbf{M}_{C1}$, and the other polarizer, $\mathbf{P}_1$. Finally, the Stokes vector at the detector, $\mathbf{S_{out}}$ is given as [10]

$$\mathbf{S}_{\text{out}} = \mathbf{P}_1\mathbf{M}_{C1}\mathbf{M}_S\mathbf{M}_{C0}\mathbf{P}_0\mathbf{S}_{\text{in}}. \tag{2}$$

2.1. Ideal Fresnel rhomb

When Fresnel rhombs perform as an ideal linear retarder, which means that retardance is only contributed from several total internal reflections, the Mueller matrix of a rotating Fresnel rhomb is given as

$$\mathbf{M}_{C_r} = \mathbf{R}(-\theta)\mathbf{M}_L(\delta_r)\mathbf{R}(\theta) \tag{3}$$

where $\mathbf{R}(\theta)$ and $\mathbf{M}_L$ represent rotation matrix and linear retarder given as

$$\mathbf{R}(\theta) = \begin{bmatrix} 1 & 0 & 0 & 0 \\ 0 & \cos 2\theta & \sin 2\theta & 0 \\ 0 & -\sin 2\theta & \cos 2\theta & 0 \\ 0 & 0 & 0 & 0 \end{bmatrix}, \tag{4}$$

and

$$\mathbf{M_L} = \begin{bmatrix} 1 & 0 & 0 & 0 \\ 0 & 1 & 0 & 0 \\ 0 & 0 & \cos\delta_r & -\sin\delta_r \\ 0 & 0 & \sin\delta_r & \cos\delta_r \end{bmatrix}, \tag{5}$$

where δ_r represents the accumulated retardance arising from total internal reflections, which most generally is a function of the wavelength and θ represents the azimuth angle of Fresnel rhomb with respect to a reference system. For a rotating compensator system, a Fresnel rhomb acting as compensator will be mounted in a motor so that this angle changes dynamically with time, and it can be written as:

$$\theta = \theta_r + \phi \tag{6}$$

where θ_r represents rotation angle of the motor, ϕ must be understood as an offset angle that indicates the orientation of the compensator with respect to the instrument's coordinate system when $\theta_r = 0$. These equations are analog to those used to describe a compensator based on a single waveplate with linear birefringence.

2.2. A stressed Fresnel rhomb

The stress-induced birefringence in the otherwise isotropic Fresnel rhomb will give rise to a refractive index ellipsoid whose principal axes align with the principal stress axes [9], and these axes may not coincide with those defined by the total internal reflections.

One possibility to describe a stressed rotating Fresnel rhomb is to use the multiplication, in a cascade, of the Mueller matrices corresponding to two or more retarders. For example, in the simplest case where we considered only the succession of a stress region followed by a total internal reflection we may write:

$$\mathbf{M}_{C_t} = \mathbf{R}(-\theta)\mathbf{M}_L(\delta_r)\mathbf{R}(-\theta_t)\mathbf{M}_L(\delta_t)\mathbf{R}(\theta_t)\mathbf{R}(\theta) \tag{7}$$

where θ_t represents the azimuth angle of stress-induced birefringence with respect to the coordinate of total internal reflection; δ_t represents the retardance from the stress along the path that light goes through.

According to Jones equivalence theorem [11], any succession of retarders can be also equivalently written as a product of a linear retarder followed by a circular retarder.

$$\mathbf{M}_{C_t} = \mathbf{R}(\bar{\rho})\mathbf{R}(-\bar{\theta})\mathbf{M}_L(\bar{\delta})\mathbf{R}(\bar{\theta}) \tag{8}$$

where $\bar{\delta}$ and $\bar{\rho}$ respectively represent the equivalent linear retardance and equivalent optical rotation angle and $\bar{\theta}$ is the equivalent azimuth angle of the compensator. This formalism was recently employed to describe compound waveplates serving as compensators [12–15]. However, it should be noted that both Eqs. (7) and (8) are order-depending, meaning that for a correct description we need a realistic assumption about the order in which the stress region and total internal reflection take place inside the rhomb which, as it is discussed in [9], can be fairly complicated.

Another possibility is to describe the stressed rotating Fresnel rhomb by a single polarization matrix, without trying to discretize the polarization transformations occurring at each region of the rhomb. According to Jones differential theory [16], any non-depolarizing optical system can be described by a general 2 × 2 Jones matrix incorporating eight polarization effects with respect to the reference coordinate system, which consists of isotropic phase retardation η, isotropic amplitude absorption k, horizontal linear birefringence LB, horizontal linear dichroism LD, 45° linear birefringence LB′, 45° linear dichroism LD′, circular birefringence CB, circular dichroism CD [17]. The most general Jones matrix is given as

$$\mathbf{J} = e^{\frac{-i\chi}{2}} \begin{bmatrix} \cos\frac{\mathrm{T}}{2} - \frac{i\mathrm{L}}{\mathrm{T}}\sin\frac{\mathrm{T}}{2} & \frac{(\mathrm{C}-i\mathrm{L}')}{\mathrm{T}}\sin\frac{T}{2} \\ -\frac{(\mathrm{C}+i\mathrm{L}')}{\mathrm{T}}\sin\frac{\mathrm{T}}{2} & \cos\frac{\mathrm{T}}{2} + \frac{i\mathrm{L}}{\mathrm{T}}\sin\frac{\mathrm{T}}{2} \end{bmatrix} \tag{9}$$

where $\mathrm{T} = \sqrt{\mathrm{L}^2 + \mathrm{L}'^2 + \mathrm{C}^2}$, $\chi \equiv 2(\eta - ik)$, $\mathrm{L} \equiv \mathrm{LB} - i\mathrm{LD}$, $\mathrm{L}' \equiv \mathrm{LB}' - i\mathrm{LD}'$ and $\mathrm{C} \equiv \mathrm{CB} - i\mathrm{CD}$. LB, LB′ and CB are related to the retardance, δ, the azimuth angle, θ, and the optical rotation angle, ρ, by

$$\mathrm{LB} = \delta\cos 2\theta \tag{10a}$$

$$\mathrm{LB}' = \delta\sin 2\theta \tag{10b}$$

$$\mathrm{CB} = 2\rho \tag{10c}$$

$\mathrm{LD}, \mathrm{LD}', \mathrm{CD}$ are related to the linear diattenuation, Ψ, and the circular diattenuation, Φ, effects that may be generated at the interfaces of the rhomb. We can express them as

$$\mathrm{LD} = \Psi\cos 2\theta \tag{11a}$$

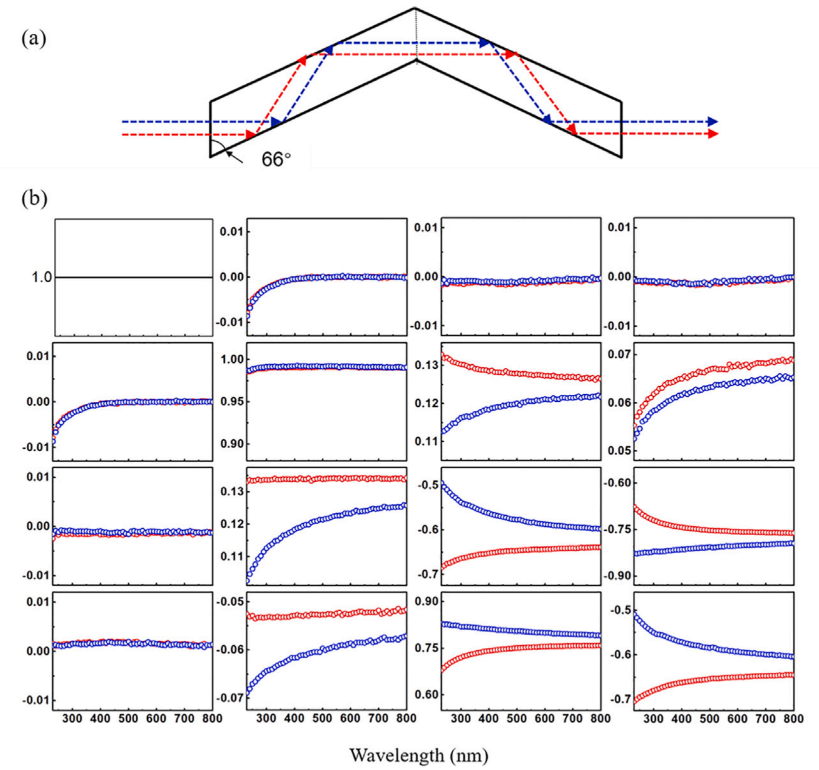

Fig. 1. (a) A fused silica Fresnel rhomb serving as a sample was installed in a holder giving slight stress and two measurements were performed for two beam positions giving slightly different paths. (b) Spectroscopically measured Mueller matrices of the Fresnel rhomb at these two different positions (blue and red circles).

$$\mathrm{LD}' = \Psi \sin 2\theta \tag{11b}$$

$$\mathrm{CD} = \Phi \tag{11c}$$

In principle, the angle, θ appearing in Eq. (11) could be not necessarily equal to the one appearing in Eq. (10), but as the main contribution to both retardation and diattenuation effects are the reflections at the interfaces of the prism it is reasonable to assume that their axes will coincide.

If the Jones matrix in Eq. (9) is directly transformed into the Mueller matrix, that formalism will be rather complex to present [18]. Fortunately, a simplification of the formalism can be easily realized by assuming vanishing or small values for the diattenuation effects.

If LD, LD′ and CD are equal to 0 (a system without diattenuation), the Mueller matrix corresponding to Eq. (9) is given as

$$\mathbf{M}_C = \begin{bmatrix} 1 & 0 & 0 & 0 \\ 0 & \cos(\mathrm{T}_R) + \mathrm{L}B^2\alpha & \mathrm{LBLB}'\alpha + \mathrm{CB}\beta & -\mathrm{LBCB}\alpha + \mathrm{LB}'\beta \\ 0 & \mathrm{LBLB}'\alpha - \mathrm{CB}\beta & \cos(\mathrm{T}_R) + \mathrm{LB}'^2\alpha & -\mathrm{LB}'^2\mathrm{CB}\alpha - \mathrm{LB}\beta \\ 0 & -\mathrm{LBCB}\alpha - \mathrm{LB}'^2\beta & -\mathrm{LB}'^2\mathrm{CB}\alpha + \mathrm{LB}\beta & \cos(\mathrm{T}_R) + \mathrm{CB}^2\alpha \end{bmatrix} \tag{12}$$

with $\alpha = (1 - \cos(\mathrm{T}_R))/\mathrm{T}_R^2$, $\beta = \sin(\mathrm{T}_R)/T_R^2$, $\mathrm{T}_R = \sqrt{LB^2 + LB'^2 + CB^2}$. Eq. (12) is functionally similar to Eq. (8) but in a single expression, that is not order-depending. If the value of CB is set to be 0, Eq. (12) will be completely equal to Eq. (3).

If diattenuation effects are nonzero but take small values, which is the expected situation in Fresnel rhombs made of transparent materials [9], Eq. (9) can be approximately transformed into the Mueller matrix

$$\mathbf{M}_C \approx \begin{bmatrix} 1 & -\mathrm{LD} & -\mathrm{LD}' & \mathrm{CD} \\ -\mathrm{LD} & \cos(T_R) + \mathrm{LB}^2\alpha & \mathrm{LBLB}'\alpha + \mathrm{CB}\beta & -\mathrm{LBCB}\alpha + \mathrm{LB}'\beta \\ -\mathrm{LD}' & \mathrm{LBLB}'\alpha - \mathrm{CB}\beta & \cos(\mathrm{T}_R) + \mathrm{LB}'^2\alpha & -\mathrm{LB}'^2\mathrm{CB}\alpha - \mathrm{LB}\beta \\ \mathrm{CD} & -\mathrm{LBCB}\alpha - \mathrm{LB}'^2\beta & -\mathrm{LB}'^2\mathrm{CB}\alpha + \mathrm{LB}\beta & \cos(\mathrm{T}_R) + \mathrm{CB}^2\alpha \end{bmatrix}. \tag{13}$$

Compared to the Mueller matrix in Eq. (12), the elements of the first column and the first row in Eq. (13) are substituted by −LD, −LD′ and CD respectively. We consider Eq. (13) as the most general Mueller matrix providing the description of the retardance, optical rotation angle, and weak diattenuation of a non-depolarizing medium. In a following section, we will discuss how this matrix can be used for the calibration of a Mueller matrix ellipsometer based on rotating Fresnel rhombs.

3. Experimental Mueller matrix of a Fresnel rhomb

To evaluate experimentally the polarization transformations introduced by the Fresnel rhomb, we used the Mueller matrix polarimeter based on 4 photoelastic modulators described in [19] to measure in the straight-through configuration the complete normalized Mueller matrix of our fused silica Fresnel rhombs over a spectral range from 230 nm to 800 nm.

The measurements shown in Fig. 1 illustrate the two slightly different results obtained when changing the position of the incident beam by around 0.5 cm in the rhomb. Our Fresnel rhomb prisms have a diameter of about 1 cm and the light beam in this instrument is about 0.15 cm in diameter, therefore by changing the position by around 0.5 cm we ensured that the trajectories of light inside the rhomb that we compared were different and did not overlap. In both measurements, the rhomb was kept in the same orientation, approximately at 90° azimuth angle with respect to the instrument's reference coordinate system.

According to Eq. (3), the description of the ideal linear retarder, the elements of the first column and the first row should completely be zero. However, m_{01} and m_{10} slightly deviate from 0 in the UV region, which has been attributed to weak diattenuation coming from total internal reflections [9]. Meanwhile, the rest elements show some differences over the whole wavelength between the two positions. This mainly happens because the small stress inside the rhomb is highly dependent on the position of the beam traveling inside the prism instead of being homogeneously distributed. Employing Eq. (13), it is

Table 1
Correlation matrix of the retardance, the offset and optical rotation angles at the wavelength of 522 nm in transmission calibration of Mueller matrix ellipsometer. δ_0, ϕ_0 and ρ_0 are the parameters of the first compensator and δ_1, ϕ_1 and ρ_1 are those of the second compensator.

Paras.	δ_0	δ_1	ϕ_0	ϕ_1	ρ_0	ρ_1
δ_0	1	−0.8865	0.4217	0.4220	0.4412	−0.4198
δ_1	−0.8865	1	−0.4162	−0.4167	−0.4359	0.4230
ϕ_0	0.4217	−0.4162	1	−0.9977	0.9987	0.9923
ϕ_1	0.4220	−0.4167	−0.9977	1	0.9987	0.9910
ρ_0	0.4412	−0.4359	0.9987	0.9987	1	−0.9969
ρ_1	−0.4198	0.4230	0.9923	0.9910	−0.9969	1

possible to calculate the polarization properties for both trajectories. For example, at the wavelength of 500 nm LD and CD are almost 0 for both paths; however, the CB of the path in red is –0.55° while that of the blue is 0.13°. The retardance δ also has a slight deviation from 130.98° (blue) to 129.89° (red) and the azimuth angles θ are, respectively, 87.81° (blue) and 87.72° (red). Thus, when the rhomb serves as a compensator in the Mueller matrix ellipsometer it needs to be calibrated in situ to ensure that light beam follows the same trajectory that during a measurement, and it is necessary to re-calibrate the system if there is some substantial deviation in the alignment of the instrument.

4. Calibration of Fresnel rhombs in Mueller matrix ellipsometers

The parameters in Eq. (13), the linear retardance δ, the offset angle ϕ, the optical rotation angle ρ, the linear diattenuation Ψ and the circular diattenuation Φ are obtained by performing a regression calibration procedure (a least squares fit) using standard samples with well-known optical response [20]. Since most parameters can be strongly wavelength-dependent due to the dispersion effect of the fused silica (the exception is the offset angle that is expected to have almost no variation with wavelength), the regression calibration procedure is performed wavelength-by-wavelength. The calibration procedure that we will describe can be executed in situ, with both rhombs mounted as rotating compensator elements when they are well aligned (so that the optical path of light inside the rhombs does not change in a substantial way as they rotate).

In our previous work [10], the calibration of PSG and PSA rhombs was fully executed using a transmission measurement with an "air" sample whose Mueller matrix is the well-known 4×4 identity matrix. However, in that work, only the retardance, δ_0 and δ_1, were considered in the calibration process. When the optical rotation angles and the offset angles are also taken into consideration in the calibration, there is a strong risk of parameter coupling if both rhombs are calibrated together from a single transmission measurement. For instance, Table 1 shows that the offset angle ϕ_0 and the optical rotation angle ρ_0 of the compensator in the PSG are strongly coupled together with maximum correlation coefficients, and at the same time, they are also coupled with the parameters ϕ_1 and ρ_1 of the second compensator. This indicates that the transmission configuration cannot be used to calibrate ϕ_0, ρ_0, ϕ_1 and ρ_1.

Here we propose a new calibration procedure where δ_0 and δ_1 are first calibrated in transmission over the whole range of wavelengths, while setting all the other parameters to constant. Then, ϕ_0, ϕ_1, ρ_0 and ρ_1 were calibrated in reflection, at the incident angle of 65° and using a $< 100 >$ silicon wafer as a sample. This reflection calibration fully relies on matrix symmetries (for this isotropic material the off-block diagonal must be zero and the remaining elements must show the well-known "Psi-Delta" symmetries), so it is not necessary to make use of the optical functions of silicon. Thus, the calibration can be done for any isotropic material that shows good reflectivity. The correlation matrix obtained from this reflection calibration, shown in Table 2, indicates that ϕ and ρ parameters are much less correlated than in the transmission case.

Table 2
Correlation matrix of the offset and optical rotation angles at the wavelength of 522 nm for the reflection calibration of Mueller matrix ellipsometer.

Parameters	ϕ_0	ϕ_1	ρ_0	ρ_1
ϕ_0	1	−0.8362	0.6628	−0.7842
ϕ_1	−0.8362	1	−0.7590	0.7535
ρ_0	0.6628	−0.7590	1	−0.4691
ρ_1	−0.7842	0.7535	−0.4691	1

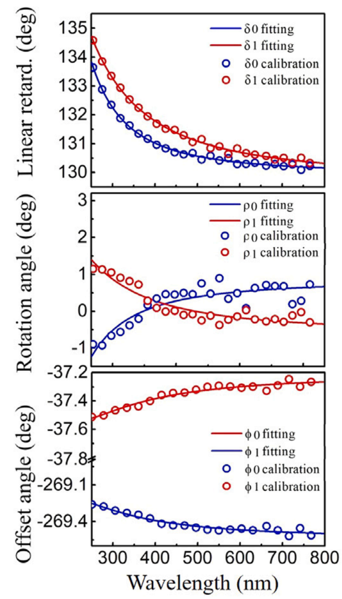

Fig. 2. Retardance, optical rotation angles, and offset angles of the two Fresnel rhombs are determined from calibration and they are fitted by Cauchy model.

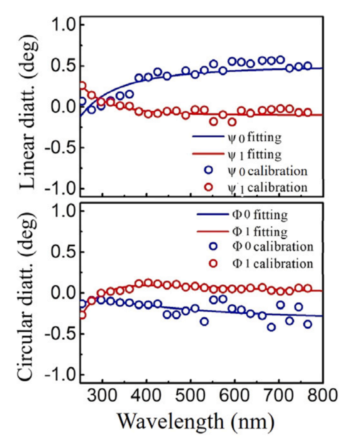

Fig. 3. Linear diattenuations (Ψ_0 and Ψ_1) and circular diattenuations (Φ_0 and Φ_1) of the two Fresnel rhomb compensators as determined from calibration. Experimental values are fitted by a Cauchy model.

Fig. 2 shows the spectroscopic values of δ, ϕ and ρ after the wavelength-by-wavelength calibration. In the final step, all of these are fitted by a Cauchy dispersion function. The linear retardance of the two Fresnel rhombs is close to the designed optimal value 132°. The optical rotation angles are much smaller, showing that the Fresnel rhombs behave as an elliptical retarder with very small ellipticity. The offset angles show less dispersion with wavelength than the other parameters, but still, there is some measurable change.

The calibration method for Fresnel rhombs that we have proposed can be most likely also applied to other types of compensators often used in Mueller matrix ellipsometry, such as achromatic retarders based

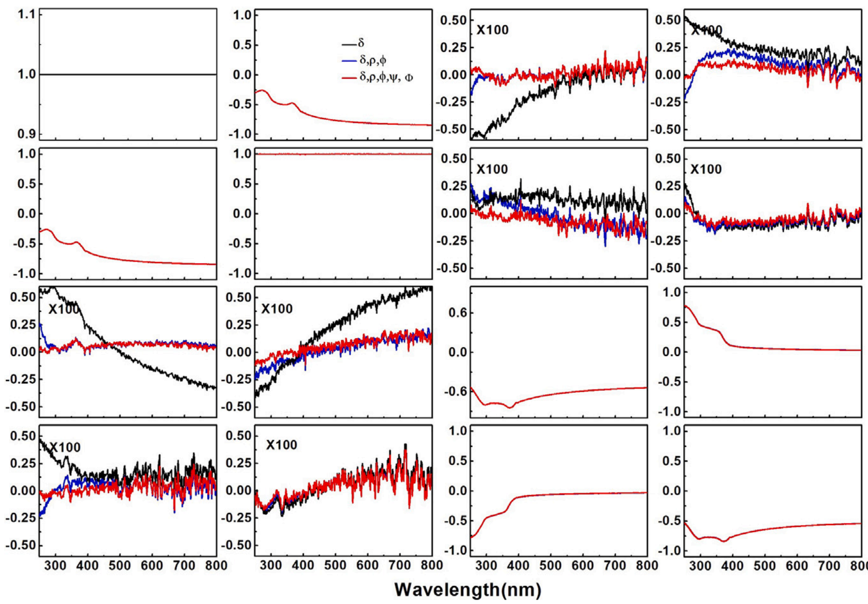

Fig. 4. Measured Mueller matrix of < 100 > plane silicon wafer when using different calibration processes. The black line corresponds to a situation where only δ parameters have been calibrated and all the other parameters are set to zero. The blue line corresponds to a calibration that adds ρ and ϕ. The red line corresponds to calibration which also considers Ψ and Φ. Off-block-diagonal elements are magnified by 100 times.

on compound waveplates. Such retarders can be also designed so that they have retardances close to the optimal one, but typically they do not reach the level of achromaticity of a Fresnel rhomb. Moreover, as the dependence of the retardance with wavelength is far more complex than for a Fresnel rhomb, their spectroscopic response cannot be modeled with a smooth curve such a Cauchy dispersion.

Finally, we also took into consideration Ψ and Φ parameters in the calibration. As these parameters were expected to have a very small value, their initial values for the fit were set to zero in the reflection calibration. Fig. 3 shows the results of the calibration and the best spectroscopic fits for these parameters. Both Ψ and Φ have a very slight deviation from zero so their overall role in the calibration process is relatively small.

Fig. 4 shows the experimental measurements of <100> plane silicon wafer after calibration where the scale of off-block-diagonal elements is magnified 100 times for a clear comparison. As expected, when only the linear retardance δ was calibrated (results shown in the black curve) obvious systematic errors occur producing the deviation of the off-block-diagonal from zero. After the ρ and ϕ parameters were incorporated into calibration, systematic errors significantly decreased, as it shown by the blue curve. When Φ and Ψ were also added to the calibration, systematic error is further improved and it reaches the best level, here shown by the red curve. After the calibration process, the accuracy of our Mueller matrix ellipsometer is better than 0.002 for all the available spectral range, while precision stays around 0.0005 in all Mueller matrix elements.

5. Conclusion

We have presented a calibration method for Mueller matrix ellipsometer based on Fresnel rhombs where the most general form of an elliptical retarder with small diattenuation is employed to describe the Fresnel rhombs. The advantage of this formalism is that both the stress-induced retardance and the small diattenuation coming from the interfaces are taken into account in the calibration, at the same time that the "intrinsic" linear retardance of the rhomb arising from total internal reflection is precisely determined. The results show that our Fresnel rhombs act as elliptical retarders with small ellipticity, which substantially depends on the stress on the prism applied by the holder. After our spectroscopic calibration of linear retardance, optical rotation, and azimuth angle the systematic errors of our Mueller matrix measurements have been significantly improved.

CRediT authorship contribution statement

Subiao Bian: Investigation, Methodology, Data curation, Writing – original draft. **Xipeng Xu:** Resources project of China administration. **Changcai Cui:** Supervision, Review. **Oriol Arteaga:** Supervision, Conceptualization, Writing – review & editing.

Declaration of competing interest

The authors declare that they have no known competing financial interests or personal relationships that could have appeared to influence the work reported in this paper.

Data availability

Data will be made available on request.

Acknowledgments

This work has been supported by Spanish Ministerio de Ciencia Innovación y Universidades, Spain through projects RYC2018-024997-I and RTI2018-098410-J-I00 (MCIU/AEI/FEDER, UE) and by Chinese government scholarship, China (Grant 202108350066).

References

[1] M.W. Davidson, Pioneers in optics: Dominique-François-Jean Arago and Augustin-Jean Fresnel, Microsc. Today 18 (1) (2010) 46–47, http://dx.doi.org/10.1017/S1551929510991207.

[2] D. Mawet, H. Charles, C. Lenaers, P. Riaud, D. Vandormael, L. Jerome, K. Fleury-Frenette, J. Plesseria, J. Surdej, S. Habraken, Fresnel rhombs as achromatic phase shifters for infrared nulling interferometry, Opt. Express 15 (20) (2007) 12850–12865, http://dx.doi.org/10.1364/OE.15.012850.

[3] A. Bertoncini, C. Liberale, Polarization micro-optics: Circular polarization from a Fresnel rhomb 3D printed on an optical fiber, IEEE Photon. Technol. Lett. PP (2018) 1, http://dx.doi.org/10.1109/LPT.2018.2871161.

[4] E. Garcia-Caurel, A. Lizana, G. Ndong, B. Al-Bugami, C. Bernon, E. Al-Qahtani, F. Rengnez, A. Martino, Mid-infrared Mueller ellipsometer with pseudo-achromatic optical elements, Appl. Opt. 54 (10) (2015) 2776–2785, http://dx.doi.org/10.1364/AO.54.002776.

[5] M. Kulish, Comparison of properties inherent to wave plates and Fresnel rhomb, Semicond. Phys., Quant. Electron. Optoelectron. 16 (5) (2013) 64–71, http://dx.doi.org/10.15407/SPQEO16.01.064.

[6] S. Hann, N. Macleod, P. Morawska, A. Dzipalski, R. Carter, I. Elder, R. Lamb, M. Esser, D. Hand, Stress induced birefringence of glass-to-metal bonded components, in: Emerging Imaging and Sensing Technologies for Security and Defence V; and Advanced Manufacturing Technologies for Micro-and Nanosystems in Security and Defence III, Vol. 11540, SPIE, 2020, pp. 113–120, http://dx.doi.org/10.1117/12.2574219.

[7] T. Vasudevan, R. Krishnan, Dispersion of the stress-optic coefficient in glasses, Br. J. Appl. Phys. 5 (12) (1972) 2283–2287, http://dx.doi.org/10.1088/0022-3727/5/12/317.

[8] H. Jensen, J. Schellman, T. Troxell, Modulation techniques in polarization spectroscopy, Appl. Spectrosc. 32 (2) (1978) 192–200, http://dx.doi.org/10.1366/000370278774331567.

[9] A. Shan, B. Ramanujam, N. Podraza, R. Collins, Analysis of non-idealities in rhomb compensators, Opt. Express 29 (22) (2021) 36328–36352, http://dx.doi.org/10.1364/OE.440680.

[10] S. Bian, C. Cui, O. Arteaga, Mueller matrix ellipsometer based on discrete-angle rotating Fresnel rhomb compensators, Appl. Opt. 60 (16) (2021) 4964–4971, http://dx.doi.org/10.1364/AO.425899.

[11] H. Hurwitz, R. Jones, A new calculus for the treatment of optical systems II. Proof of three general equivalence theorems, J. Opt. Soc. Amer. 31 (7) (1941) 493–499, http://dx.doi.org/10.1364/JOSA.31.000493.

[12] D. Gottlieb, O. Arteaga, Optimal elliptical retarder in rotating compensator imaging polarimetry, Opt. Lett. 46 (13) (2021) 3139–3142, http://dx.doi.org/10.1364/OL.430266.

[13] D. Gottlieb, O. Arteaga, Mueller matrix imaging with a polarization camera: Application to microscopy, Optics Express 29 (21) (2021) 34723–34734, http://dx.doi.org/10.1364/OE.439529.

[14] H. Gu, X. Chen, Y. Shi, H. Jiang, C. Zhang, P. Gong, S. Liu, Comprehensive characterization of a general composite waveplate by spectroscopic Mueller matrix polarimetry, Opt. Express 26 (19) (2018) 25408–25425, http://dx.doi.org/10.1364/OE.26.025408.

[15] H. Gu, H. Jiang, X. Chen, C. Zhang, S. Liu, Superachromatic polarization modulator for stable and complete polarization measurement over an ultra-wide spectral range, Opt. Express 30 (9) (2022) 15113–15133, http://dx.doi.org/10.1364/OE.456290.

[16] R.C. Jones, A new calculus for the treatment of optical systems. VII. Properties of the N-matrices, J. Opt. Soc. Amer. 38 (8) (1948) 671–685, http://dx.doi.org/10.1364/JOSA.38.000671.

[17] O. Arteaga, A. Canillas, Analytic inversion of the Mueller-Jones polarization matrices for homogeneous media, Opt. Lett. 35 (4) (2010) 559–561, http://dx.doi.org/10.1364/OL.35.000559.

[18] O. Arteaga, Mueller matrix polarimetry of anisotropic chiral media, (Ph.D. thesis), Universitat de Barcelona, 2010.

[19] O. Arteaga, J. Freudenthal, B. Wang, B. Kahr, Mueller matrix polarimetry with four photoelastic modulators: theory and calibration, Appl. Opt. 51 (28) (2012) 6805–6817, http://dx.doi.org/10.1364/AO.51.006805.

[20] H. Gu, X. Chen, H. Jiang, C. Zhang, S. Liu, Optimal broadband mueller matrix ellipsometer using multi-waveplates with flexibly oriented axes, J. Opt. 18 (2) (2016) 025702, http://dx.doi.org/10.1088/2040-8978/18/2/025702.